ISSN 1814-4225 (print)
ISSN 2663-2012 (online)

UDC 629.7.014.16. **doi: 10.32620/aktt.2026.3.09**

Vitalii DZHULGAKOV, Dmytro SOKOL

National Aerospace University "Kharkiv Aviation Institute", Kharkiv, Ukraine

NONLINEAR QUADROTOR MODELING: FROM ANALYTICAL DERIVATION TO PHYSICAL SIMULATION

*The **subject matter** of this study is the expansion of an H-frame quadrotor mathematical model to include nonlinearities and the implementation of its dynamics within the Simscape Multibody simulation environment. The **goal** is to develop a comprehensive nonlinear motion model and verify its accuracy by comparing analytical descriptions with physics-based component modeling. The **tasks** to be solved are: to analyze the challenges of describing and implementing nonlinear quadrotor models; to formulate a system of nonlinear differential equations using the Euler–Lagrange formalism; to conduct simulation experiments on the initial mathematical model; to develop and integrate a physical rigid-body model into the automatic control system; to perform a comparative analysis of the results. **Methods** are used: the Euler–Lagrange formalism, numerical methods, and comparative statistical analysis. The following **results** were obtained: a refined nonlinear mathematical model of an H-frame quadrotor was developed, accounting for cross-coupled gyroscopic effects and electromechanical actuator dynamics. A dynamic model based on physical constraints and inertia tensors was implemented in Simscape Multibody. Maneuvering scenarios for both the mathematical and multi-domain models indicate characteristic transients for orientation angles within the [11, 15] s interval. It was determined that the steady-state deviation for the mathematical model is 0.1° for yaw and roll and 0.12° for pitch, while the maximum error over the simulation interval reached 2.4° for yaw, 0.1° for roll, and 0.15° for pitch. Corresponding indicators for the multi-domain model were: a steady-state deviation of 1° for yaw, 0.9° for roll, and 1.3° for pitch, with maximum errors of 3°, 0.9°, and 1.3°, respectively. These values result from natural error accumulation due to different kinematic parameterization methods, gyroscopic moments, and electromechanical dynamics. **Conclusions**. The scientific novelty of the results obtained is as follows: the scientific and methodological approach to assessing the fidelity of complex dynamic systems was further developed, which, unlike existing ones, is based on the cross-platform verification of the analytical Euler–Lagrange formalism and multi-domain simulation; this allowed for the first time to establish the applicability limits of nonlinear models and to quantitatively determine the error in reproducing flight scenario caused by specific kinematic parameterization and cross-coupling dynamics. Quantitative evaluation confirmed the fidelity of both models. The steady-state deviations between the two models are 0.9° (yaw), 0.8° (roll), and 1.2° (pitch); at maximum error, they are 4.2° (yaw), 0.8° (roll), and 1.23° (pitch). Utilizing Simscape physical components significantly simplifies frame parameter modification, process visualization, and the formulation of coupling equations, as the tool handles part of the model implementation. The proposed approach provides a high-fidelity virtual prototype for testing robust control algorithms under conditions close to real-world operation.*

Keywords: *quadrotor; control system; nonlinear dynamics; Euler–Lagrange formalism; multi-domain simulation.*

1. Introduction

1.1. Motivation

In modern robotics, quadrotors have become a fundamental and well-established subject of control theory, widely utilized for military missions [1], search and rescue operations [2], surface monitoring [3], logistics [4], and aerial photography [5]. While the standard dynamic equations describing the general behavior of such systems are thoroughly developed and universally accepted in the academic community, current technological advancements demand performance far beyond classical stabilization and positioning in idealized environments. Modern applications involve biomimetic [6] and flapping-wing systems [7], UAVs capable of adaptive transformation under wind loads [8], and high-precision autonomous navigation [9]. In this context, dynamic equations are no longer merely a preliminary research result but have evolved into a critical tool integrated into complex, multi-level control and navigation frameworks.

To effectively address applied engineering challenges, a quadrotor's mathematical model must account for specific operational nuances and remain compatible with integrated subsystems, such as LiDAR-based control [10] and Computer Vision technologies [11]. The traditional iterative design approach involves sequential parameter refinement; however, incorporating the

maximum number of physical factors and initial data at the early design stages significantly enhances the final product's quality and reduces resource consumption. Current practices often rely on simplified assumptions during the modeling phase, necessitating costly corrections after extensive field or semi-natural experiments. A more rational approach involves the a priori inclusion of known nonlinear characteristics and physical parameters within the model. This is particularly crucial for developing nonlinear robust fast terminal sliding mode controllers [12], neural network-based architectures [13], and adaptive robust control under conditions of uncertainties in the system [14].

Admittedly, increasing the level of detail in a mathematical description leads to an inherent escalation in model complexity. However, modern computer-aided engineering and multi-domain simulation technologies allow for an effective balance, ensuring high fidelity without compromising the development process's efficiency. This paper examines the expansion of a quadrotor mathematical model to include specific nonlinearities and its subsequent implementation within the Simulink Simscape environment [15]. The primary focus is placed on deriving a system of nonlinear differential equations using the Euler–Lagrange formalism and integrating rigid body dynamics into a physical simulation environment. This approach facilitates a transition to multi-domain modeling – combining rigorous mathematical descriptions with physical component connections – thereby streamlining parameter estimation and enhancing analytical capabilities through intuitive 3D visualization.

1.2. Objectives and tasks

The primary objective of this study is the development and verification of a refined nonlinear quadrotor dynamic model integrated into a multi-domain simulation environment to enhance the fidelity of dynamic process reproduction. Achieving this objective involves solving several interrelated tasks based on a transition from abstract mathematical assumptions to physics-oriented design.

The implementation methodology relies on the Simscape environment, which constitutes a key feature of the proposed approach. Instead of the traditional programming of dynamic functions as closed "black-box" blocks, this work proposes implementing quadrotor dynamics as a rigid body system using physical components. This approach enables:

– establishing direct physical connections between inertial characteristics, frame geometry, and motor thrust vectors;

– integrating the mechanical assembly with automatic control systems within a unified computational framework;

– conducting a comparative analysis between results obtained via two applied methods.

The underlying iterative process aims to minimize discrepancies between the theoretical model and the physical object. It is hypothesized that utilizing verifiable physical parameters during the design stage eliminates the need for excessive model simplification for the sake of computational efficiency, while maintaining the precision required for synthesizing high-performance control algorithms.

Thus, the approach is based on the principle of moving from complex descriptions to intuitive implementation, where the complexity of the mathematical apparatus is balanced by the clarity and functionality of modern software suites.

The fundamental research framework combines analytical methods of classical mechanics with advanced integrated simulation tools. The mathematical basis of this work is built upon the Euler-Lagrange equations, allowing for the derivation of a rigorous system of nonlinear differential equations that describe the vehicle's dynamics as a 6-DOF system. In contrast to linearized models, this framework fully accounts for cross-coupling between control channels, as well as aerodynamic and gyroscopic moments occurring during high-intensity maneuvering.

To achieve the goal, within the framework of this publication it is necessary to solve the following tasks:

– conduct a critical analysis of existing approaches to the implementation of nonlinear mathematical models in UAV simulation;

– derive a rigorous system of nonlinear differential equations for a quadrotor using the Euler-Lagrange formalism;

– implement the dynamics of the quadrotor as a rigid body using physical components in a multi-domain simulation environment;

– conduct a comparative analysis of the results obtained from both the analytical and physical models to validate the fidelity of the proposed approach.

The article is structured as follows:

Section 2 describes the objectives and methodology, detailing the transition from abstract mathematical assumptions to physics-oriented design. It presents the derivation of the comprehensive nonlinear mathematical model, including kinematics and rigid body dynamics. In the end it focuses on the actuation system modeling and the electromechanical characteristics of the motor-ESC units. It details the computer implementation in Simulink and the preliminary simulation results. The alternative multi-domain implementation using Simscape Multibody are described.

Section 3 provides a comparative analysis of the results and a discussion of the observed discrepancies.

Section 4 concludes the article by summarizing the conclusions and providing prospects for further research.

2. Materials and methods of research

The formulation of a mathematical model necessitates the analysis of physical models through rigorous analytical frameworks. For the design and simulation of quadrotor control systems, the Lagrangian approach is particularly advantageous, as it systematically handles mechanical systems with multiple degrees of freedom [16].

This method inherently incorporates energy components – kinetic and potential – from which the dynamic equations are derived. Furthermore, the Lagrangian formalism is directly applicable to the synthesis of model-based controllers.

2.1. Quadrotor kinematics and dynamics

Prior to defining the mathematical model of the quadrotor dynamics, the following assumptions and initial conditions were established:

– aerodynamic drag is neglected for the initial derivation;

– the Earth is considered an inertial reference frame;

– all coordinate systems are defined using the right-handed East-North-Up (ENU) convention;

– the orientation angles follow a specific convention: yaw and roll angles increase according to the right-hand rule (yaw – counter-clockwise rotation, roll – tilt to the right), while the pitch angle is defined such that "nose up" corresponds to a positive displacement (following a left-handed convention for this specific axis).

The physical configuration of the H-frame quadrotor is illustrated in Fig. 1.

Physical model contains:

– $wx_gy_gz_g$ is the inertial reference frame;

– $OXYZ$ is the body-fixed frame;

– x, y, z are the coordinate of the center of mass (CoM) of the quadrotor;

– ϕ, θ, ψ are the roll, pitch and yaw angles;

– ω_i is the rotor angular velocity;

– a, b, c are length, width and height of the quadrotor;

– d is the length of the arm;

– h is the vertical displacement between the propeller plane and OXY;

– r is the propeller radius;

– F_i is the propeller thrust;

– M_{Fi} is the electric drive torque;

– M_{di} is the propeller drag moment;

– M_{sti} is the static moment of resistance in the electric drive.

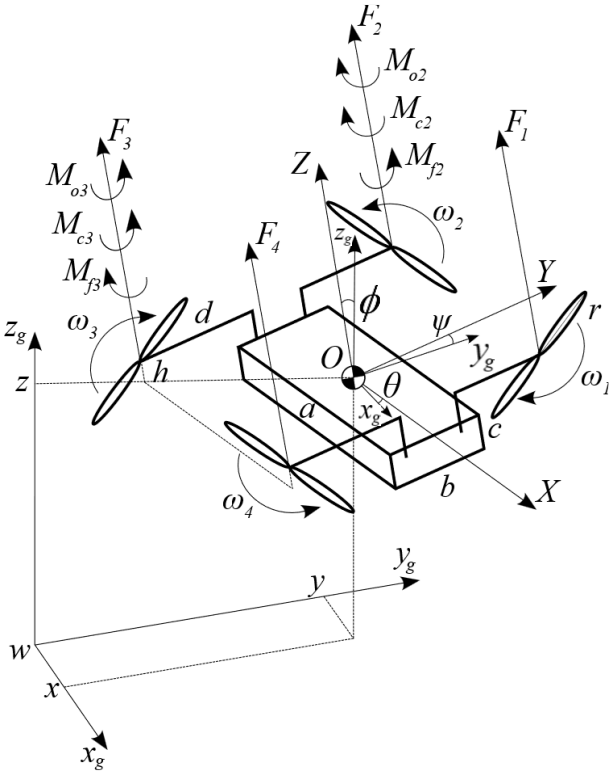

Fig. 1. Physical configuration of the H-frame quadrotor

The moments are illustrated in Fig. 1 for arms 2 and 3; however, arms 1 and 4 possess an identical set of moments with corresponding directions.

The Euler-Lagrange equation is employed to derive the mathematical model of the quadrotor:

$$\frac{\mathrm{d}}{\mathrm{dt}}\left(\frac{\partial \mathrm{L}}{\partial \dot{\mathrm{q}}_\mathrm{i}}\right) - \frac{\partial \mathrm{L}}{\partial \mathrm{q}_\mathrm{i}} = \mathrm{Q}_\mathrm{i}, \tag{1}$$

where L is the Lagrangian;

q_i is the generalized coordinate;

Q_i is the generalized force.

The motion is characterized by 6-DOF, which uniquely define its position and orientation in the inertial reference frame:

$$\mathrm{q} = \begin{bmatrix} \mathrm{x} & \mathrm{y} & \mathrm{z} & \phi & \theta & \psi \end{bmatrix}^\mathrm{T}. \tag{2}$$

The linear velocity in the inertial frame is defined as

$$\mathrm{v} = \begin{bmatrix} \dot{\mathrm{x}} \\ \dot{\mathrm{y}} \\ \dot{\mathrm{z}} \end{bmatrix} \tag{3}$$

and the angular velocity in the body-fixed frame is defined as follows

$$\omega = \begin{bmatrix} \omega_x \\ \omega_y \\ \omega_z \end{bmatrix} = B(\phi, \theta) \begin{bmatrix} \dot{\phi} \\ \dot{\theta} \\ \dot{\psi} \end{bmatrix}, \quad (4)$$

where the transformation matrix

$$B = \begin{bmatrix} 1 & 0 & -\sin\theta \\ 0 & \cos\phi & \sin\phi\cos\theta \\ 0 & -\sin\phi & \cos\phi\cos\theta \end{bmatrix} \quad (5)$$

maps the Euler angular rates to the body angular velocity vector according to the Z-Y-X "passive" rotation sequence.

Consequently, the inverse relationship representing the kinematic coupling between angles and rates is given by:

$$\begin{bmatrix} \dot{\phi} \\ \dot{\theta} \\ \dot{\psi} \end{bmatrix} = B^{-1}(\phi, \theta) \begin{bmatrix} \omega_x \\ \omega_y \\ \omega_z \end{bmatrix} = \\ = \begin{bmatrix} 1 & \sin\phi\,\mathrm{tg}\theta & \cos\phi\,\mathrm{tg}\theta \\ 0 & \cos\phi & -\sin\phi \\ 0 & \dfrac{\sin\phi}{\cos\theta} & \dfrac{\cos\phi}{\cos\theta} \end{bmatrix} \begin{bmatrix} \omega_x \\ \omega_y \\ \omega_z \end{bmatrix}. \quad (6)$$

The kinetic energies of translational and rotational motion can now be defined:

$$T_t = \frac{1}{2} m v^T v; \quad (7)$$

$$T_r = \frac{1}{2} \omega^T I \omega, \quad (8)$$

where $I = \mathrm{diag}(I_{xx}, I_{yy}, I_{zz})$ is the quadrotor moment of inertia tensor;

m is the total weight of the quadrotor.

It is crucial to note that for a configuration where thrust F_i is perfectly aligned with the OZ axis and aerodynamic drag is neglected, vertical displacement h does not explicitly enter the torque equations.

However, in such a scenario, the mass distribution varies such that the inertia of each motor relative to the CoM increases.

According to the Huygens-Steiner Parallel Axis theorem, the diagonal elements of the moment of inertia tensor for the quadrotor as a solid rectangular cuboid are derived as:

$$\begin{cases} I_{xx} = \dfrac{m_b}{12}(b^2 + c^2) + m_i(d^2 + 4h^2); \\ I_{yy} = \dfrac{m_b}{12}(a^2 + c^2) + m_i(d^2 + 4h^2); \\ I_{zz} = \dfrac{m_b}{12}(a^2 + b^2) + 2m_i d^2, \end{cases} \quad (9)$$

where m_b, m_i are the body and arm mass, respectively.

Evidently, vertical displacement h increases the moments of inertia for the roll I_{xx} and pitch I_{yy} axes quadratically. This indicates that as the rotor plane rises above the CoM, the resistance to attitude changes increases, necessitating larger control moments to maintain the same angular acceleration. Conversely, the yaw inertia I_{zz} remains independent of h, as the distance between the motors and the OZ axis is determined solely by d.

The total kinetic energy as the sum of (7) and (8):

$$T = T_t + T_r = \frac{1}{2} m(\dot{x}^2 + \dot{y}^2 + \dot{z}^2) + \frac{1}{2} \omega^T I \omega. \quad (10)$$

The potential energy, with the CoM as the reference point, depends only on the altitude in the inertial reference frame:

$$U = mgz. \quad (11)$$

The Lagrangian is defined as the difference between the total kinetic (10) and potential (11) energies:

$$L = T - U = \\ = \frac{1}{2} m(\dot{x}^2 + \dot{y}^2 + \dot{z}^2) + \frac{1}{2} \omega^T I \omega - mgz. \quad (12)$$

Within the context of the Euler–Lagrange framework, generalized forces Q_i describe external non-conservative influences performing work on the system. The quadrotor is modeled as a rigid body whose dynamics are driven by the total propeller thrust along OZ axis:

$$F_B = \sum_{i=1}^{4} F_i \quad (13)$$

and the control moments around the body axes

$$M_B = \begin{bmatrix} M_\phi & M_\theta & M_\psi \end{bmatrix}^T. \quad (14)$$

The thrust is defined as a function of the propellers' angular velocities:

$$F_i = k_F \omega_i^2, \quad (15)$$

where k_F is the propeller thrust coefficient.

Since thrust F_i acts along the body OZ axis, it must be mapped to the stationary inertial frame:

$$F_I = R(\phi, \theta, \psi)\begin{bmatrix}0 & 0 & F_B\end{bmatrix}^T, \quad (16)$$

where $R = R_z R_y R_x$ is the rotation matrix.

Given the axis orientations and the established positive angular conventions, the elementary rotation matrices are:

$$R_x(\phi) = \begin{bmatrix}1 & 0 & 0\\ 0 & \cos\phi & -\sin\phi\\ 0 & \sin\phi & \cos\phi\end{bmatrix};$$
$$R_y(\theta) = \begin{bmatrix}\cos\theta & 0 & -\sin\theta\\ 0 & 1 & 0\\ \sin\theta & 0 & \cos\theta\end{bmatrix}; \quad (17)$$
$$R_z(\psi) = \begin{bmatrix}\cos\psi & -\sin\psi & 0\\ \sin\psi & \cos\psi & 0\\ 0 & 0 & 1\end{bmatrix}.$$

The result of equation (16) is the vector in the inertial frame:

$$F_I = \begin{bmatrix}Q_x & Q_y & Q_z\end{bmatrix}^T. \quad (18)$$

Using the Z-Y-X rotation sequence, the components of the generalized forces are expressed as:

$$\begin{cases}Q_x = F_B(\sin\phi\sin\psi - \cos\phi\sin\theta\cos\psi);\\ Q_y = F_B(-\sin\phi\cos\psi - \cos\phi\sin\theta\sin\psi);\\ Q_z = F_B\cos\phi\cos\theta.\end{cases} \quad (19)$$

For angular coordinates, the generalized forces are the moments. Roll Q_ϕ and pitch Q_θ moments are generated by the thrust differential, while the yaw force Q_ψ is determined by the torque balance on the motor shafts:

$$\begin{cases}Q_\phi = \frac{d}{2}k_F(\omega_1^2 + \omega_2^2 - \omega_3^2 - \omega_4^2);\\ Q_\theta = \frac{d}{2}k_F(\omega_1^2 - \omega_2^2 - \omega_3^2 + \omega_4^2);\\ Q_\psi = k_m(\omega_1^2 - \omega_2^2 + \omega_3^2 - \omega_4^2),\end{cases} \quad (20)$$

where k_m is the propeller drag coefficient.

Solving the Euler-Lagrange equations (1) yields the translational dynamics:

$$m\begin{bmatrix}\ddot{x}\\ \ddot{y}\\ \ddot{z}\end{bmatrix} = R(\phi, \theta, \psi)\begin{bmatrix}0\\ 0\\ F_B\end{bmatrix} - \begin{bmatrix}0\\ 0\\ mg\end{bmatrix}, \quad (21)$$

which can be represented in terms of linear acceleration:

$$\begin{cases}\ddot{x} = \frac{F_B}{m}(\sin\phi\sin\psi - \cos\phi\sin\theta\cos\psi);\\ \ddot{y} = \frac{F_B}{m}(-\sin\phi\cos\psi - \cos\phi\sin\theta\sin\psi);\\ \ddot{z} = \frac{F_B}{m}\cos\phi\cos\theta - g.\end{cases} \quad (22)$$

Equation of the dynamics of rotational motion can be formulated as:

$$\begin{cases}I_{xx}\dot{\omega}_x - (I_{yy} - I_{zz})\omega_y\omega_z = Q_\phi;\\ I_{yy}\dot{\omega}_y - (I_{zz} - I_{xx})\omega_z\omega_x = Q_\theta;\\ I_{zz}\dot{\omega}_z - (I_{xx} - I_{yy})\omega_x\omega_y = Q_\psi,\end{cases} \quad (23)$$

The gyroscopic moment in quadrotor dynamics is a "parasitic" effect arising from the angular momentum of the rapidly spinning propellers. When the airframe tilts (changes in ϕ or θ), the rotor's axis of rotation changes its orientation in space. According to the laws of mechanics, this induces a reaction moment perpendicular to both the rotor's axis and the body's angular velocity vector.

Each rotor acts as a gyroscope. Given the body's angular velocity, the gyroscopic moment is determined by the vector cross-product:

$$M_{gyro,i} = I_{rot}(\Omega \times e_z\omega_i), \quad (24)$$

where $e_z = \begin{bmatrix}0 & 0 & 1\end{bmatrix}^T$ is the vector of the axis of propeller rotation in the body-fixed frame;

$I_{rot} \approx \frac{1}{3}m_i r^2$ is the total moment of inertia of the rotor and propeller.

In the body-fixed frame, the projections of the total gyroscopic moment from all four rotors onto the OX and OY axes are as follows:

$$\begin{cases}M_{gyro,\phi} = I_{rot}\omega_y(\omega_1 - \omega_2 + \omega_3 - \omega_4);\\ M_{gyro,\theta} = I_{rot}\omega_x(\omega_2 - \omega_1 + \omega_4 - \omega_3).\end{cases} \quad (25)$$

This system of equations reflects the fact that in

level flight, the net gyroscopic moment is zero. Incorporating these terms, the right-hand sides of the angular dynamic equations (23) take the following form:

$$\begin{aligned} \ldots &= Q_\phi + M_{gyro,\phi}; \\ \ldots &= Q_\theta + M_{gyro,\theta}. \end{aligned} \tag{26}$$

Thus, a complete system of nonlinear differential equations has been obtained, describing the quadrotor dynamics as a rigid body.

2.2. Actuation subsystem

The executive subsystem of the quadrotor comprises J2514 1500 KV brushless DC (BLDC) motors paired with APD 80F3[X] electronic speed controllers (ESC). The standard mathematical representation of a BLDC motor integrates both electrical and mechanical dynamics. The electrical behavior of the J2514 motor is governed by the following voltage balance equation:

$$L\frac{di}{dt} + Ri + k_e\omega = U, \tag{27}$$

where u is the ESC voltage; i is the current flowing through the windings; R is the winding resistance; L is the inductance; k_e is the back EMF coefficient.

The mechanical dynamics of the J2514 motor, in its generalized form, are expressed as:

$$I_{rot}\frac{d\omega}{dt} = M_m - M_l, \tag{28}$$

where M_m is the motor torque;

M_l is the propeller load moment.

To refine the mechanical equations (27, 28), the moments illustrated in Fig. 1 are utilized: M_{Fi} is the electromagnetic torque generated by the motor, acting as the primary driver of motion, M_{di} is the aerodynamic load resulting from the viscous friction of the propellers against the air, M_{sti} is the combined dry and viscous friction within the bearings that opposes rotation.

Consequently, the comprehensive electromechanical system for the motor is formulated as:

$$I_{rot}\dot{\omega}_i = M_{Fi} - M_{di} - M_{sti}. \tag{29}$$

For the BLDC, the electromagnetic torque is defined as:

$$M_F = k_t i, \tag{30}$$

where k_t is the electromagnetic torque constant.

The aerodynamic drag moment of the propeller is modeled as:

$$M_d = k_m\omega^2. \tag{31}$$

The static drag moment within the electric drive supports (bearings) is given by:

$$M_{st} = M_{dry} + \eta\omega, \tag{32}$$

where M_{dry} is the dry friction moment;

η is the coefficient of viscous friction in bearings.

The transition from the high-fidelity physical motor model to its representation as a control unit is defined as:

$$\begin{cases} \dfrac{di_i}{dt} = \dfrac{1}{L_i}\left(U_i - R_i i_i - k_e\omega_i\right); \\ \dfrac{d\omega_i}{dt} = \dfrac{1}{I_{roti}}\left(k_t i_i - k_m\omega_i^2 - \left(M_{dryi} + \eta\omega_i\right)\right). \end{cases} \tag{33}$$

To establish the final relationship between the generalized forces Q_i and the control signals u_i – thereby completing the quadrotor's full dynamic model – the ESC must be characterized. The ESC converts the input PWM signal into an average phase voltage U_i. Accounting for the inherent delays associated with PWM switching and signal filtering τ_{esc}, the ESC dynamics are modeled as a first-order aperiodic link:

$$\tau_{esc}\frac{dU_i}{dt} + U_i = k_{esc}u_i. \tag{34}$$

The derived mathematical model, encompassing both the 6-DOF rigid body dynamics and the electromechanical characteristics of the actuation system, provides a rigorous foundation for the subsequent development of the high-fidelity multi-domain simulation.

3. Computer-Aided Modeling and Simulation

3.1. Mathematical-based simulation

The structure of the quadrotor computer model, including its actuation elements, is shown in Fig. 2. This version is implemented in the Simulink environment and is based strictly on the derived differential equations, organized into the Actuation subsystem and the Quadrotor dynamics (Fig. 3).

ISSN 1814-4225 (print)
АВІАЦІЙНО-КОСМІЧНА ТЕХНІКА І ТЕХНОЛОГІЯ, 2026, № 3(211) ISSN 2663-2012 (online)

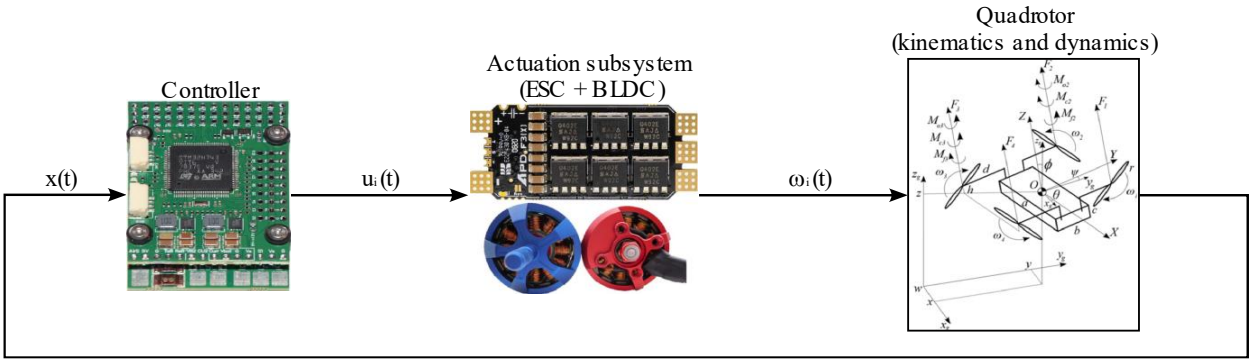

Fig. 2. Overall connection diagram of the quadrotor computer model based on mathematical equations

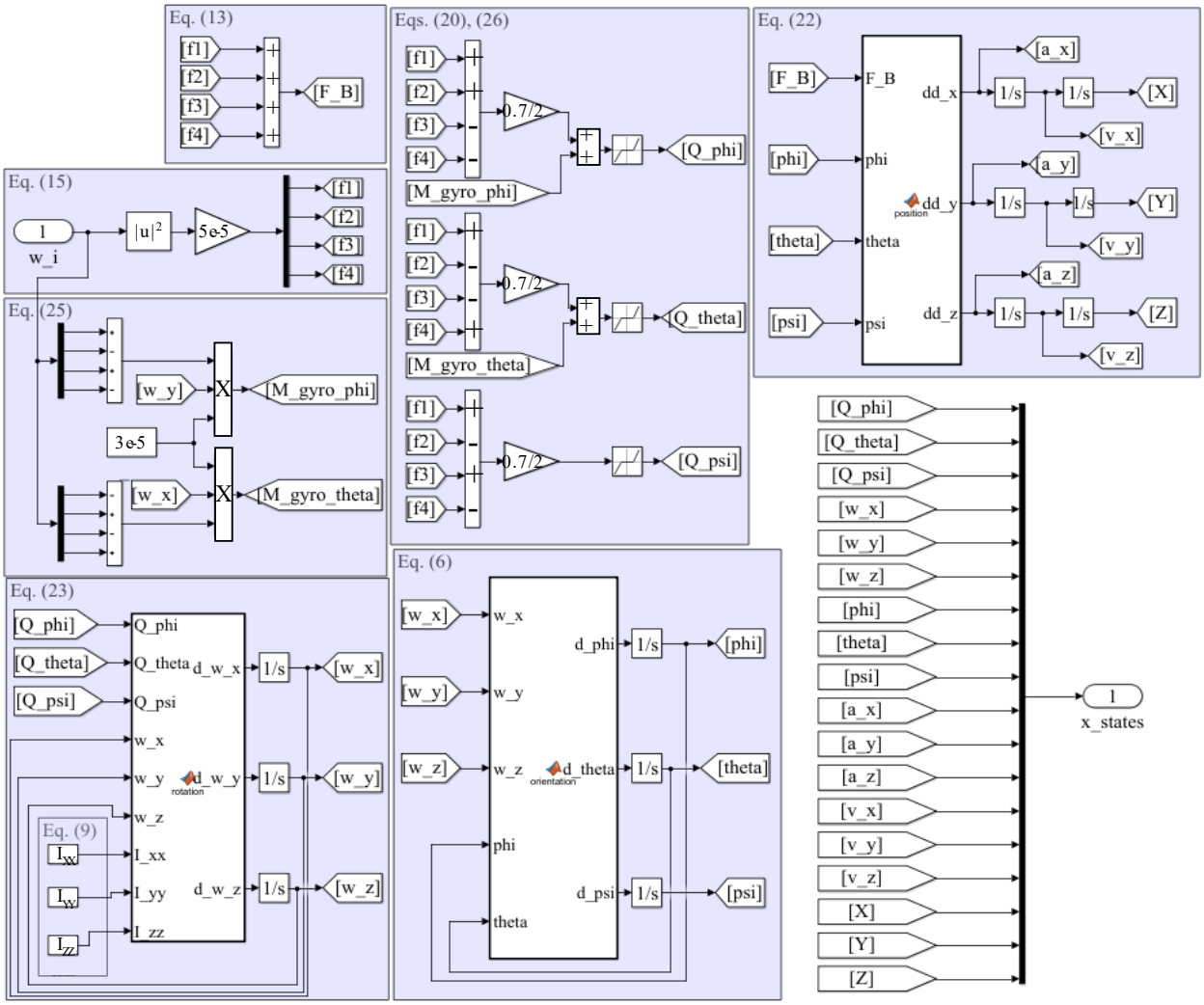

Fig. 3. Structure of the Quadrotor subsystem

The Controller subsystem (Fig. 4) performs the following functions: command generation for the desired flight trajectory, implementation of multi-loop (nested) control laws, and computation of the control allocation matrix.

The reference commands are generated considering signal constraints tailored to the operational requirements of a low-maneuverability H-frame quadrotor: maximum altitude of 50 m, roll and pitch angles restricted to [-45, +45]°, and a yaw rate within [-90, 90]°/s.

Furthermore, the pitch angle constraint prevents the gimbal lock phenomenon inherent in the kinematic equation (6).

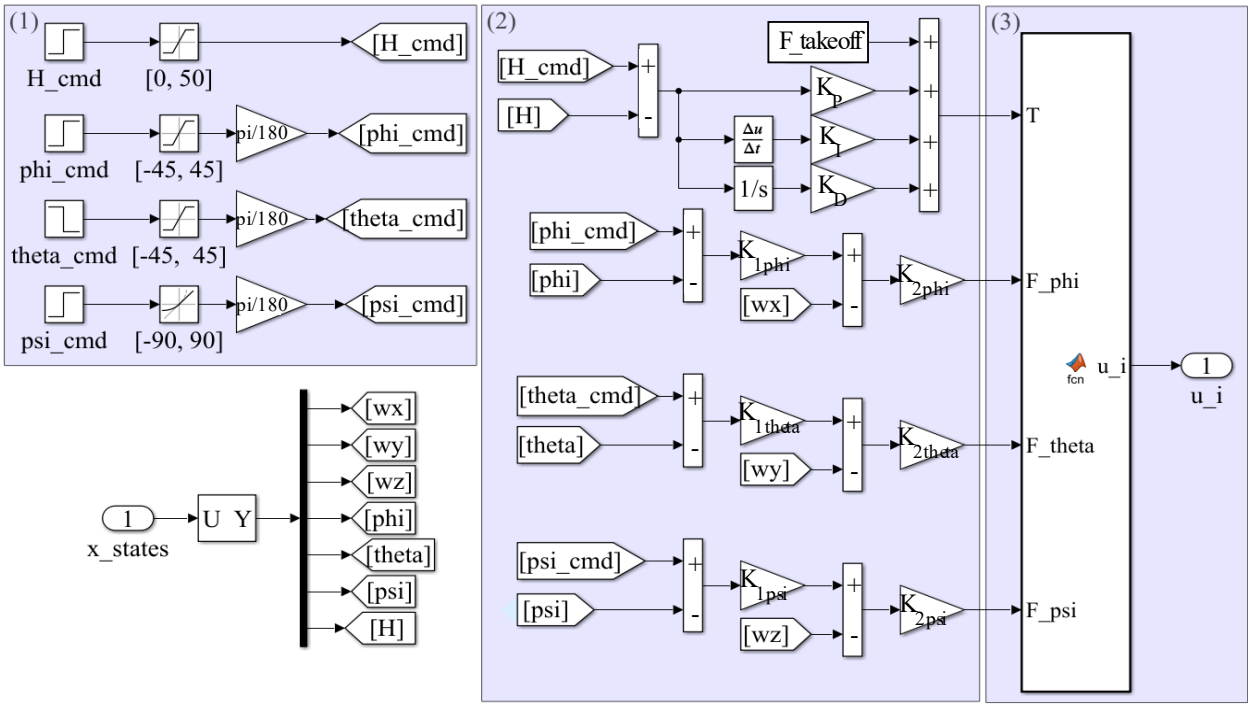

Fig. 4. Structure of the Controller subsystem

The multi-loop architecture consists of classical regulators for each channel: altitude controller

$$F_{cmd} = F_{takeoff} + k_P \Delta H + k_I \Delta \dot{H} + k_D \int \Delta H dt, \quad (35)$$

and orientation controllers:

$$\begin{cases} \hat{F}_\phi = k_{\phi,2}\left(k_{\phi,1}\Delta\phi - \omega_x\right); \\ \hat{F}_\theta = k_{\theta,2}\left(k_{\theta,1}\Delta\theta - \omega_y\right); \\ \hat{F}_\psi = k_{\psi,2}\left(k_{\psi,1}\Delta\psi - \omega_z\right), \end{cases} \quad (36)$$

where $\Delta H = H_{cmd} - H$;

$\Delta\phi = \phi_{cmd} - \phi$;

$\Delta\theta = \theta_{cmd} - \theta$;

$\Delta\psi = \psi_{cmd} - \psi$;

$F_{takeoff}$ is the thrust for taking-off;

$\hat{F}_\phi$, $\hat{F}_\theta$, $\hat{F}_\psi$ are estimated roll, pitch and yaw forces.

The control allocation matrix translates the desired moments into estimated thrust values for individual rotors according to equation (20).

$$\begin{bmatrix} \hat{F}_1 \\ \hat{F}_2 \\ \hat{F}_3 \\ \hat{F}_4 \end{bmatrix} = \begin{bmatrix} 1/4 & 1/d & 1/d & 1/4k_m \\ 1/4 & 1/d & -1/d & -1/4k_m \\ 1/4 & -1/d & -1/d & 1/4k_m \\ 1/4 & -1/d & 1/d & -1/4k_m \end{bmatrix} \begin{bmatrix} \hat{F}_B \\ \hat{F}_\phi \\ \hat{F}_\theta \\ \hat{F}_\psi \end{bmatrix}, \quad (37)$$

The Controller subsystem generates control voltages with appropriate saturation limits for these thrusts:

$$u_i \in [0,1] \Rightarrow F_i \in [0, F_{max}], \quad (38)$$

ensuring realistic commands from the controller.

The physical constants and parameters are summarized in Table 1.

Table 1

Physical constants and parameters

Parameter	Value	Parameter	Value
m , kg	5.6	I_{rot} , kg/m^2	$3\cdot10^{-5}$
m_b , kg	2.4	L , H	0.0001
m_i , kg	0.8	R , Om	0.15
a , m	0.7	k_e , V/(rad·s)	$6.4\cdot10^{-3}$
b , m	0.35	k_t , (N·m)/A	$6.4\cdot10^{-3}$
c , m	0.15	k_m	$1.5\cdot10^{-6}$
d , m	0.7	k_F	$5\cdot10^{-5}$
h , m	0.15	η , (N·s)/m	$2\cdot10^{-6}$
I_{xx} , kg/m^2	0.5	M_{dry} , N·m	0.0002
I_{yy} , kg/m^2	0.57	k_{esc}	22.2
I_{zz} , kg/m^2	0.9	τ_{esc} , s	0.02

The simulation results for a specific flight scenario are presented in Fig. 5. The scenario includes: vertical ascent to 5 m (0 s), then yaw rotation of 90° (5 s), then roll rotation of 30° (10 s), pitch rotation of -15° (11 s).

ISSN 1814-4225 (print)
ISSN 2663-2012 (online)

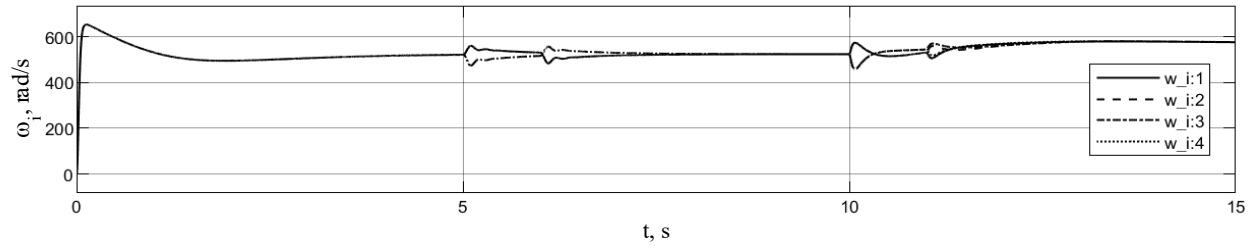

a

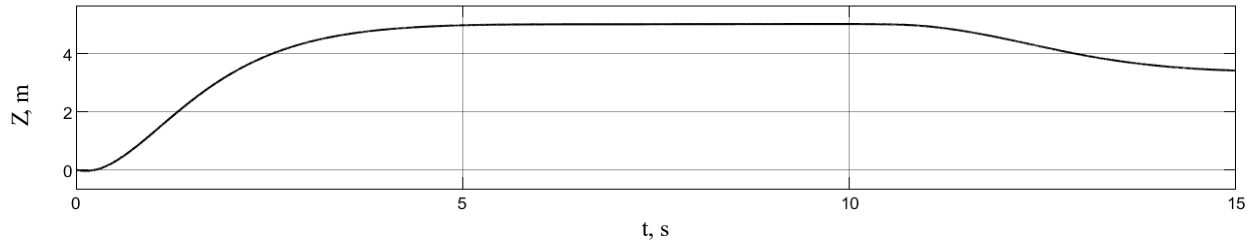

b

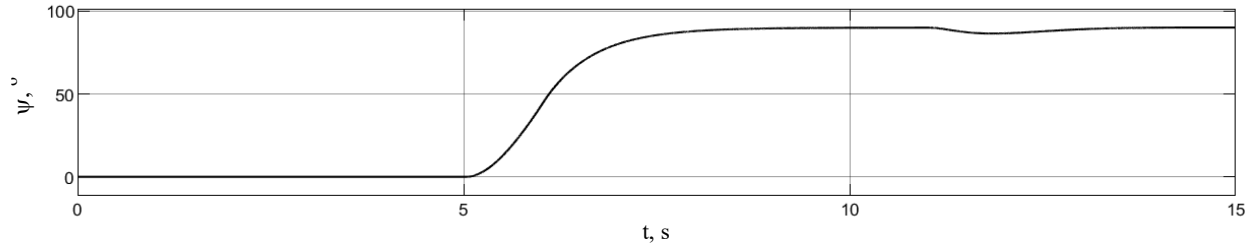

c

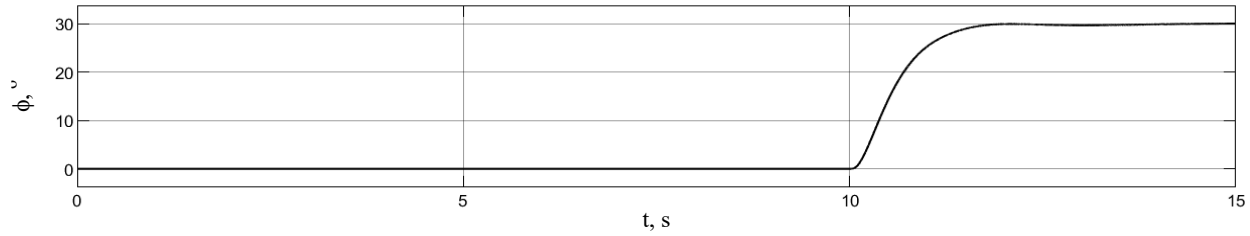

d

e

Fig. 5. Experimental results for the prescribed flight scenario:
a – rotor angular velocities; b – altitude; c – yaw; d – roll; e – pitch

According to the plots, all rotors rotate at a uniform speed to lift the vehicle to 5 m (Fig. 5a). The angular velocity peaks at 650 rad/s before stabilizing at 520 rad/s, allowing the quadrotor to reach the target altitude in 5 s (Fig. 5b).

Subsequently, a 90° yaw rotation is executed without altitude loss; this is achieved by increasing the speeds of rotors 1 and 3 while decreasing rotors 2 and 4, maintaining constant total thrust. The yaw maneuver is completed within 3 s (Fig. 5c). At 10 s, the roll angle changes to 30° (Fig. 5d), followed by a pitch adjustment to -15° at 11 s (Fig. 5e).

The influence of gyroscopic moments is evident across all plots during these maneuvers. Fig. 4a illustrates the corresponding adjustments in rotor angular velocities. Accounting for the compensation of gyroscopic effects, the quadrotor reaches the desired attitude in about 4 s.

The observed behavior aligns with the characteristics of the nonlinear mathematical model, providing a verified baseline for the transition to an alternative multi-domain implementation.

3.2. Multi-domain simulation

To provide an alternative implementation of the flight dynamics, specifically the rigid-body orientation, a physical model of the quadrotor was developed using the Simscape Multibody environment.

In this approach, a rigid body was constructed by integrating geometry, inertia, mass properties, and a graphical component. The detailed quadrotor assembly serves as a high-fidelity visual shell, with parameters strictly corresponding to the values specified in Table 1. Consequently, the differential equations describing the mechanical dynamics are replaced by the integrated tools of the physical simulation environment.

The architecture of the multi-domain computer model and the internal configuration of the Quadrotor (Physical model) subsystem are illustrated in Fig. 6.

A rigid interaction is established between the new Quadrotor (dynamics) physical subsystem and a simplified Quadrotor (kinematics) subsystem based on the mathematical model. The mathematical subsystem continues to compute the generalized forces Q_i, which are then transmitted as input signals to the physical model. The physical model, acting as a rigid body, adjusts its orientation accordingly and feeds back the orientation angles and angular velocities to the kinematics subsystem to determine the quadrotor's position in inertial space. The Controller and Actuation subsystems remain identical to the previous implementation to ensure consistency.

To evaluate the multi-domain model, an experiment was conducted using the same flight scenario as previously described. The results are demonstrated through the visual orientation of the physical model at key timestamps (Fig. 7).

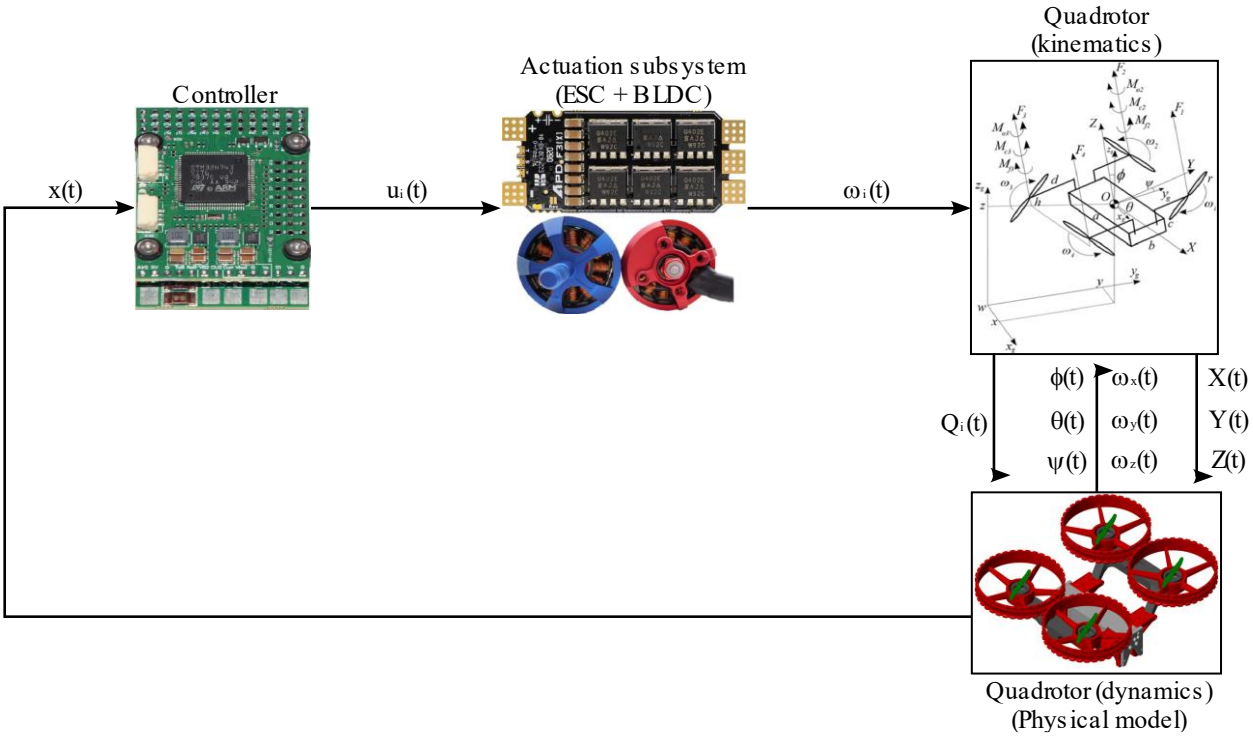

Fig. 6. Structure of the multi-domain quadrotor computer model

ISSN 1814-4225 (print)
ISSN 2663-2012 (online)

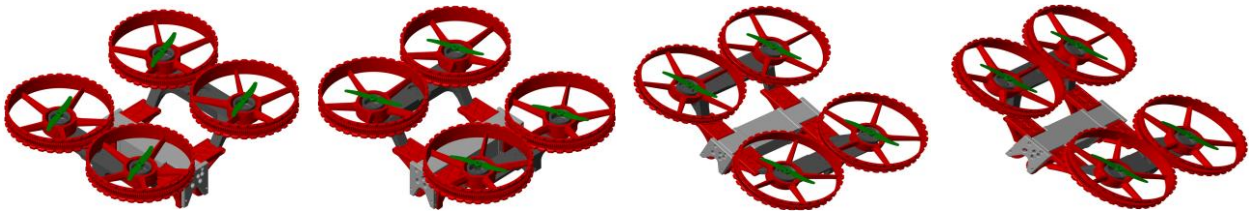

a b c d

Fig. 7. Visual orientation of the physical quadrotor model at key simulation milestones: a – prior to yaw rotation (5 s); b – post-yaw rotation and prior to roll maneuver (10 s); c – during roll rotation and prior to pitch maneuver (11 s); d – post-pitch rotation (15 s)

The transition to a multi-domain simulation environment effectively bridges the gap between abstract mathematical derivations and physical system realization, providing a robust platform for verifying nonlinear dynamics through integrated physical constraints and real-time visual feedback.

4. Results and Discussion

Simscape Multibody enables the extraction of internal sensing signals directly from the physical model components. To evaluate the consistency between the mathematical model (Fig. 2) and the multi-domain model (Fig. 6), the transient characteristics of the orientation angles were compared (Fig. 8). The rotor speeds and altitude plots are omitted here, as they are computed by identical mathematical subsystems and perfectly replicate the results shown in Fig. 5a and Fig. 5b.

Preliminary analysis of the yaw and roll variations indicates that discrepancies between the two models primarily emerge following the activation of gyroscopic moments. Consequently, a detailed comparative analysis was conducted for the interval [11, 15] s, where these nonlinear effects are most prominent. The quantitative data is summarized in Table 2.

Table 2

Quantitative comparative analysis of the quadrotor orientation configuration

Angle	Indicator	Fig. 2	Fig. 5	Error
Yaw	Deviation	0.1°	1°	0.9°
	Max. error	2.4°	3°	4.2°
Roll	Deviation	0.1°	0.9°	0.8°
	Max. error	0.1°	0.9°	0.8°
Pitch	Deviation	0.12°	1.3°	1.2°
	Max. error	0.15°	1.3°	1.23°

The observed deviations between the analytical and multi-domain models can be attributed to several factors. The most significant discrepancies occur during simultaneous multi-axis rotations. While the mathematical model accounts for gyroscopic effects through explicit cross-product terms in the Euler-Lagrange equations, Simscape Multibody computes these effects implicitly through the recursive Newton-Euler algorithm applied to the rigid body's inertia tensor. The divergence in both magnitude and sign of the error (Fig. 8) suggests that the physical simulation environment captures higher-order inertial interactions that may be simplified in the analytical derivation.

The mathematical model utilizes a standard rotation matrix based on Euler angles, which is susceptible to trigonometric singularities. In contrast, Simscape Multibody typically employs quaternion parameterization for internal computations. The necessary transformation between these coordinate representations for visualization and control introduces minor numerical residues, contributing to the total error margin.

Unlike the explicit ODE-based implementation in Simulink, the multi-domain model involves a topological analysis of the physical assembly. The difference in how the solver handles algebraic loops and stiff physical constraints in Simscape compared to the purely differential approach in the mathematical model results in the observed transient offsets.

In conclusion, while the linear controller maintains stability, it does not compensate for the inherent nonlinear differences between the two modeling approaches. However, the high degree of correlation between the results confirms that the developed nonlinear mathematical model is a valid representation of the quadrotor's physical dynamics.

4. Conclusions

The research presented in this paper successfully demonstrates the development and verification of a refined nonlinear mathematical model for an H-frame quadrotor, bridging the gap between theoretical analytical derivations and practical multi-domain simulation. By employing the Euler-Lagrange formalism, a rigorous 6-DOF dynamic framework was established, accounting for critical nonlinearities such as gyroscopic moments

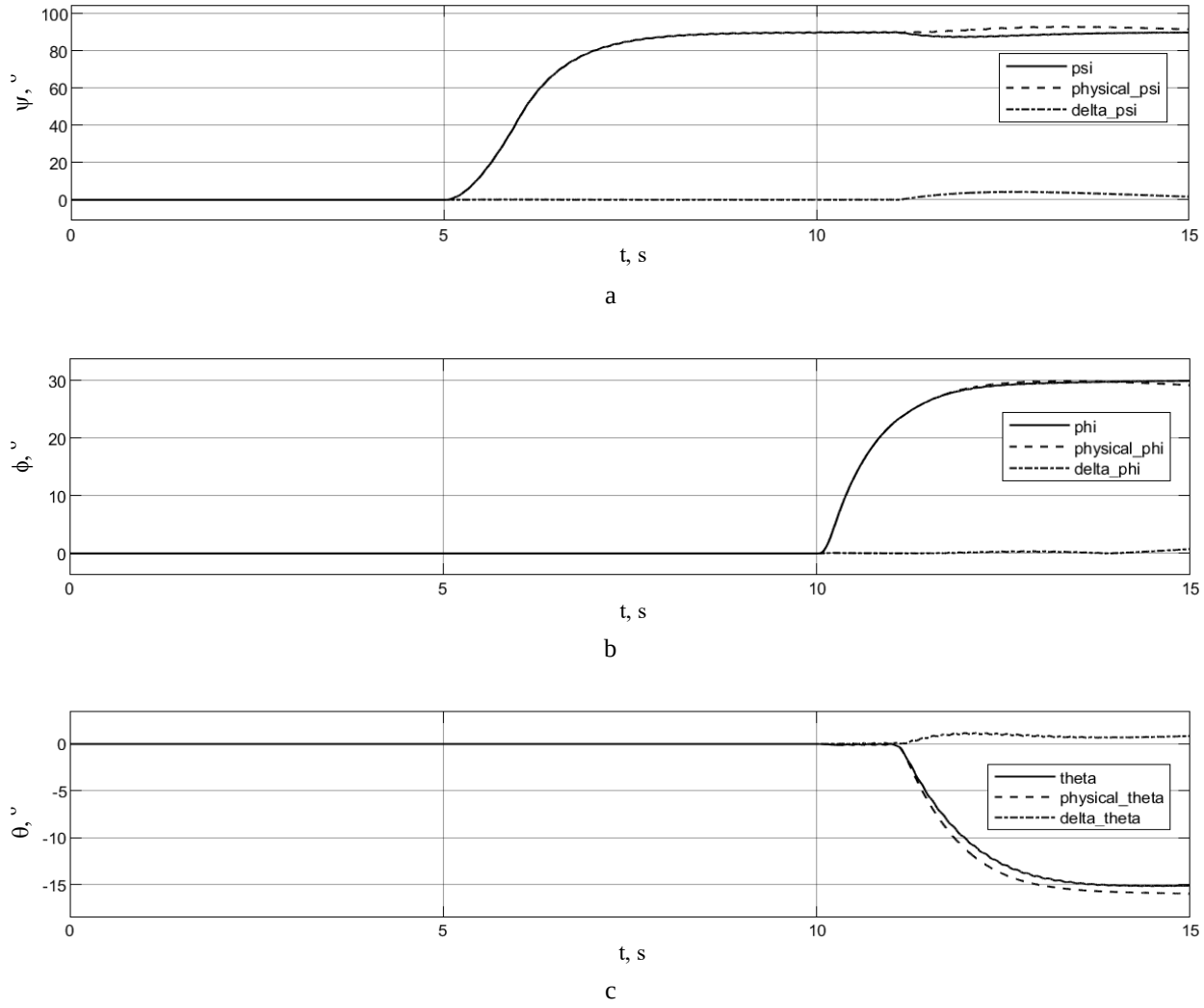

Fig. 8. Comparison of experimental results for the prescribed flight scenario:
— – model Fig. 2 (analytical); --- – model Fig. 6 (Simscape); -.-.- – difference between models;
a – yaw; b – roll; c – pitch

and complex electromechanical interactions within the actuation system. The subsequent implementation of this model in a Simscape Multibody environment provided a robust platform for comparative analysis, where the physical modeling approach validated the analytical findings through high-fidelity visual and numerical feedback.

The observed discrepancies between the two modeling methodologies, particularly during high-intensity maneuvers involving simultaneous multi-axis rotations, highlight the sensitivity of quadrotor dynamics to inertial cross-coupling and kinematic parameterization. While the analytical model provides a transparent basis for control law synthesis, the multi-domain approach offers superior capabilities for verifying physical constraints and sensor integration without the need for excessive mathematical simplification. Ultimately, the high degree of correlation between the two implementations confirms the validity of the proposed nonlinear model as a reliable foundation for the development of advanced robust control strategies. The prospects for further research lie in the synthesis of nonlinear control laws, such as Sliding Mode Control and Backstepping, which require the precise mathematical descriptions derived in this study to ensure stability under uncertainty. Furthermore, the developed multi-domain framework provides a scalable environment for investigating the quadrotor's behavior under complex environmental disturbances, including wind gusts and payload variations, as well as for implementing Hardware-in-the-Loop testing of real-time flight controllers.

Contributions of authors: research concept and design, collection and assembly of data, data analysis and interpretation, critical revision of the article – **Vitalii Dzhulgakov**; research concept and design, writing the article, data analysis and interpretation – **Dmytro Sokol.**

Conflict of Interest

The authors declare that they have no conflict of interest in relation to this research, whether financial, personal, author ship or otherwise, that could affect the research and its results presented in this paper.

Financing

This study was conducted without financial support.

Data Availability

The work has associated data that can be provided upon reasonable request.

Use of Artificial Intelligence

The authors confirm that they did not use artificial intelligence methods while creating the presented work.

All the authors have read and agreed to the published version of this manuscript.

References

1. Fedorovich, O., Popov, A., Pisklova, T., Malieiev, L., Rybka, A., Fedorovich, V. Modeling the life cycle reduction for the rapid development of UAVs for use in military missions. *Aerospace Technic and Technology*, 2026, no. 1 (209), pp. 95-107. DOI: https://doi.org/10.32620/aktt.2026.1.09 .

2. Damanik, I., Dermawan, J. A., Sitanggang, I. M., Hutabarat, F. S., Boy Knight, G. P., Sagala, A. Quadcopter Unmanned Aerial Vehicle (UAV) Design for Search and Rescue (SAR). *International Conference of Computer Science and Information Technology (ICOSNIKOM)*, Laguboti, North Sumatra, Indonesia, IEEE, 2022, pp. 1-6. DOI: https://doi.org/10.1109/ICOSNIKOM56551.2022.10034866

3. Sun, J., Yuan, G., Song, L., Zhang, H. Unmanned aerial vehicles (UAVs) in landslide investigation and monitoring: A review. *Drones*, 2024, vol. 8, no. 1(30). 27 p. DOI: https://doi.org/10.3390/drones8010030

4. Zhang, H., Zou, L., Yang, Y., Ma, J., Xiao, J., Lin, P. Urban Medical Emergency Logistics Drone Base Station Location Selection. Drones, 2026, vol. 10, no. 1 (17), 36 p. DOI: https://doi.org/10.3390/drones10010017 .

5. Tsekhmystro, R., Rubel, O., Lukin, V. Study of the dependence of accuracy in vehicles search on the size of the object using UAV images. *Aerospace Technic and Technology*, 2024, no. 3 (195), pp. 89-98. DOI: https://doi.org/10.32620/aktt.2024.3.08 .

6. Tanaka, S., Asignacion, A., Nakata, T., Suzuki, S., Liu, H. Review of biomimetic approaches for drones. *Drones*, 2022, vol. 6, no. 11 (320), 15 p. DOI: https://doi.org/10.3390/drones6110320 .

7. Liu, T., Wang, S., Liu, H., He, G. Engineering perspective on bird flight: Scaling, geometry, kinematics and aerodynamics. *Progress in Aerospace Sciences*, 2023, vol. 142. 47 p. DOI: https://doi.org/10.1016/j.paerosci.2023.100933 .

8. Vourtsis, C., Rochel, V. C., Müller, N. S., Stewart, W., Floreano, D. Wind defiant morphing drones. *Advanced Intelligent Systems*, 2023, vol. 5, iss. 3. 8 p. DOI: https://doi.org/10.1002/aisy.202200297 .

9. Lou, H., Wu, Q., Wang, H., Li, M., Liu, H., Sun, N. Structure, Modeling, and Control of Morphing Quadrotors: A Review. *International Journal of Precision Engineering and Manufacturing*, 2026, vol. 27, pp. 825-842. DOI: https://doi.org/10.1007/s12541-025-01405-4 .

10. Liu, W., Ren, Y., Guo, R., Kong, V. W. W., Hung, A. S. P., Zhu, F., Cai, Y. Slope inspection under dense vegetation using LiDAR-based quadrotors. *Nature Communications*, 2025, vol. 16. 14 p. DOI: https://doi.org/10.1038/s41467-025-62801-y .

11. Gomathi, P., Deena Rose, D., Sampath Kumar, R., Sathya Priya, M., Dinesh, S., Ramarao, M. Computer Vision for Unmanned Aerial Vehicles in Agriculture: Applications, Challenges, and Opportunities. *The Scientific Temper*, 2023, vol. 14, iss. 3, pp. 957-962. DOI: https://doi.org/10.58414/SCIENTIFICTEMPER.2023.14.3.61 .

12. Derrouaoui, S. H., Bouzid, Y., Guiatni, M. Nonlinear Robust Control of a New Reconfigurable Unmanned Aerial Vehicle. *Robotics*, 2021, vol. 10, iss. 2. 13 p. DOI: https://doi.org/10.3390/robotics10020076 .

13. Nguyen, N. P., Mung, N. X., Thanh, H. L. N. N., Huynh, T. T., Lam, N. T., Hong, S. K. Adaptive Sliding Mode Control for Attitude and Altitude System of a Quadcopter UAV via Neural Network. *Access IEEE*, 2021, vol. 9, pp. 40076-40085. DOI: https://doi.org/10.1109/ACCESS.2021.3064883 .

14. Dong, F., Yuan, B., Zhao, X., Ding, Z., Chen, S. Adaptive robust constraint-following control for morphing quadrotor UAV with uncertainty: a segmented modeling approach. *Journal of the Franklin Institute*, 2024, vol. 361, iss. 5. 15 p. DOI: https://doi.org/10.1016/j.jfranklin.2024.106678 .

15. Moustafa, E. N., Kamezaki, M., Miyake, S., Sugano, S. A Quadrotor With a New 3-DOF Hybrid Manipulator for Pipeline Maintenance: Design, Modeling, and Task-Space Control. *Access IEEE*, 2025, vol. 13, pp. 198102-198124, DOI: https://doi.org/10.1109/ACCESS.2025.3633759 .

16. Djizi, H., Zahzouh, Z., Bouzaouit, A. Quadcopter Prototype Stability Assessment With Pid Controller And Euler-Lagrange Approach. *The Scientific Bulletin of Electrical Engineering Faculty, Valahia University of Targoviste*, 2023, vol. 23, iss. 1, pp. 15-20. DOI: https://doi.org/10.2478/sbeef-2023-0003 .

Received 02.05.2026, Received in revised form 09.06.2026
Accepted date 15.06.2026, Published date 17.06.2026

НЕЛІНІЙНЕ МОДЕЛЮВАННЯ КВАДРОКОПТЕРА: ВІД АНАЛІТИЧНОГО ВИВЕДЕННЯ ДО ФІЗИЧНОГО МОДЕЛЮВАННЯ

В. Г. Джулгаков, Д. В. Сокол

Предметом вивчення в статті є розширення математичної моделі квадрокоптера з Н-подібною рамою шляхом урахування нелінійностей та реалізація його динаміки в середовищі моделювання Simscape Multibody. **Метою** є створення комплексної нелінійної моделі руху квадрокоптера та верифікації її точності через порівняльний аналіз аналітичних описів з фізично-орієнтованим моделюванням компонентів. **Завдання**: провести аналіз проблем опису та реалізації нелінійних моделей квадрокоптера; сформувати систему нелінійних диференціальних рівнянь квадрокоптера за допомогою формалізму Ейлера–Лагранжа; провести імітаційні експерименти на базовій математичній моделі; розробити та інтегрувати фізичну модель квадрокоптера як твердого тіла в загальну систему автоматичного управління; виконати порівняльний аналіз отриманих результатів. **Методи** розв'язання задач: формалізм Ейлера–Лагранжа, чисельні методи інтегрування, методи порівняльного статистичного аналізу. Отримано такі **результати**: розроблено уточнену нелінійну математичну модель квадрокоптера з Н-подібною рамою, яка враховує перехресні гіроскопічні зв'язки та динаміку електромеханічних приводів. У середовищі Simscape Multibody реалізовано динамічну модель, засновану на фізичних зв'язках і тензорах інерції. Результати сценарію маневрування для обох типів моделей вказують на характерні перехідні процеси за кутами орієнтації на інтервалі [11, 15] с. Встановлено, що статична похибка для математичної моделі становить 0.1° для кутів рискання та крену і 0.12° для тангажу, тоді як максимальне відхилення склало 2.4° для рискання, 0.1° для крену та 0.15° для тангажу. Відповідні показники для багатодоменної моделі: статична похибка – 1° для рискання, 0.9° для крену, 1.3° для тангажу; максимальне відхилення – 3°, 0.9° та 1.3° відповідно. Такі значення зумовлені природним накопиченням похибки через використання різних методів кінематичної параметризації, проявом гіроскопічних моментів та специфікою динаміки електромеханічних елементів. **Висновки**. Наукова новизна отриманих результатів полягає в наступному: дістав подальший розвиток науково-методичний підхід до оцінювання адекватності складних динамічних систем, який, на відміну від існуючих, базується на крос-платформній верифікації аналітичного формалізму Ейлера–Лагранжа та багатодоменного моделювання. Це дозволило вперше встановити межі застосовності нелінійних моделей та кількісно визначити похибку відтворення сценарію польоту, спричинену специфікою кінематичної параметризації та динамікою перехресних зв’язків. Кількісна оцінка підтвердила адекватність обох моделей: різниця у статичних похибках між ними становить 0.9° для рискання, 0.8° для крену та 1.2° для тангажа, а у максимальних відхиленнях – 4.2°, 0.8° та 1.23° відповідно. Використання фізичних компонентів Simscape значно спрощує модифікацію параметрів рами, візуалізацію процесів, оскільки інструментарій автоматизує запис рівнянь взаємних зв'язків. Запропонований підхід забезпечує створення високоточного віртуального прототипу для тестування робастних алгоритмів управління в умовах, наближених до реальної експлуатації.

Ключові слова: квадрокоптер; система управління; нелінійна динаміка; формалізм Ейлера-Лагранжа; багатодоменне моделювання.

Джулгаков Віталій Георгійович – ст. викл. каф. систем управління літальних апаратів, Національний аерокосмічний університет «Харківський авіаційний інститут», Харків, Україна.

Сокол Дмитро Вадимович – PhD, доц. каф. систем управління літальних апаратів, Національний аерокосмічний університет «Харківський авіаційний інститут», Харків, Україна.

Vitalii Dzhulgakov – Senior Lecturer at the Department of Aircraft Control Systems, National Aerospace University «Kharkiv Aviation Institute», Kharkiv, Ukraine,
e-mail: v.dzhulgakov@khai.edu, ORCID: 0000-0002-7586-1927.

Dmytro Sokol – PhD, Associate Professor at the Department of Aircraft Control Systems, National Aerospace University «Kharkiv Aviation Institute», Kharkiv, Ukraine,
e-mail: d.sokol@khai.edu, ORCID: 0000-0003-0847-350X.